

Trovacenyl-Based Organometallic Triradicals: Spin Frustration, Competing Interactions and Redox Splitting

O. Schiemann¹, J. Plackmeyer¹, J. Fritscher¹, J. Pebler²,
and C. Elschenbroich²

¹ Institut für Physikalische und Theoretische Chemie, J. W. Goethe-Universität,
Frankfurt am Main, Germany

² Fachbereich Chemie, Philipps-Universität, Marburg, Germany

Received October 9, 2003; revised November 10, 2003

Abstract. Two new triradicals based on trovacene $[(\eta^7\text{-tropylium})\text{vanadium}(\eta^5\text{-cyclopentadienyl})]$, 1,3,5-tri([5]trovacenyl)benzene **4** and 1,3,5-tri([5]trovacenyl)-6-methoxybenzene **5** were prepared and their magnetic properties were studied by continuous-wave X-band electron paramagnetic resonance (EPR) spectroscopy and by temperature-dependent magnetic susceptibility. The EPR spectra of **4** and **5** in liquid toluene solution demonstrate that the three unpaired electrons localized on the vanadium atoms interact with each other in both complexes. The data from magnetic susceptibility revealed that the electron spins in both triradicals are antiferromagnetically coupled despite the *meta*-phenylene bridge. The exchange coupling constants are equal in the C_3 -symmetrical triradical **4** ($J = J' = -0.68 \text{ cm}^{-1}$), which leads to a twofold degenerate spin ground state (spin frustration). The symmetry lowering by methoxy substitution of the benzene spacer in **5** results in the effect of competing interactions ($J = -1.83 \text{ cm}^{-1}$ and $J' = -2.38 \text{ cm}^{-1}$). In addition to magnetocommunication, the effect of ring substitution on electrocommunication is also discernable. It manifests itself in disparate redox splittings $\delta E_{1/2}$ ($0/-$, $-2/-$) and $\delta E_{1/2}$ ($-2/-$, $2/-3-$) for **5**, while these parameters are equal for the C_3 -symmetrical trinuclear complex **4**.

1 Introduction

The basis for bulk and molecular magnetic phenomena is the electron spin-spin exchange coupling between unpaired electrons, expressed by the constant J . The correlation of this exchange coupling with structural parameters is a long-standing research topic [1] which is important for the design of new magnetic materials [2] and the understanding of certain biological systems [3]. Therefore, numerous experimental and theoretical studies on bi-, tri- and oligoradicals have been devoted to the study of the dependence of J on structural parameters [4, 5]. An extensively used concept for the synthesis of bi-, tri- or oligoradicals is to connect stable organic radicals, e.g., nitroxides [6], inorganic coordination complexes, e.g., vanadyl derivatives [7], or organometallic compounds [8], e.g.,

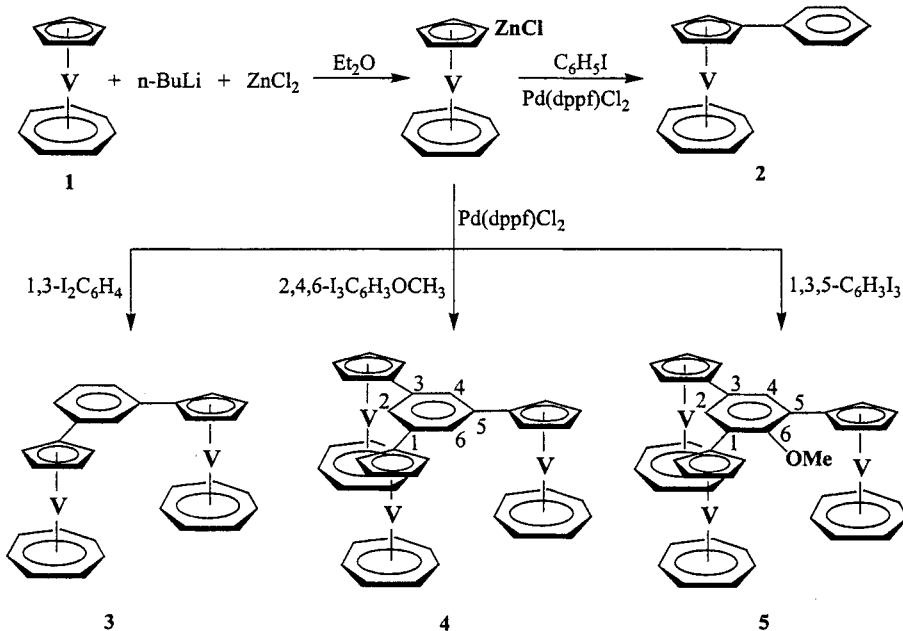


Fig. 1. Synthesis scheme.

trovacene **1** [$(\eta^7\text{-tropylium})\text{vanadium}(\eta^5\text{-cyclopentadienyl})$] (Fig. 1) [9], via different organic [10] or inorganic [11] bridges. *Meta*-substituted phenylene groups, for example, are widely used as bridges in the design of ferromagnetically coupled radicals [12–14]. It was, however, found in some cases that *meta*-phenylene derivatives can also display antiferromagnetically coupled ground states [15–17], pointing to the fact that the acquired knowledge does not yet allow an unequivocal understanding of the magneto-structural correlations. In a series of studies on these correlations we used the sandwich complex **1** as the spin-bearing group [18–23]. Compared with other organometallic bis(arene)metal compounds **1** has the following advantages: (1) the redox potential $E_{1/2}(+/0) = +0.26$ V renders **1** almost air-stable, whereas its isomer bis($\eta^6\text{-benzene})\text{vanadium}$ with $E_{1/2}(+/0) = -0.35$ V is much more sensitive to oxygen [22], (2) **1** is easily functionalized since it can be selectively lithiated at the cyclopentadienyl ring (meaning a proton is substituted by a lithium ion) [24] and (3) the neutral $\text{V}(\text{d}^5)$ complex has an orbitally nondegenerate ground state ${}^2\text{A}_1$ in which the nonbonding singly occupied molecular orbital (SOMO) is constituted to over 90% by the vanadium 3d_{z^2} orbital [22]. This contrasts with the isoelectronic ferricinium ion ($\text{Fe}(\text{d}^5)$, ${}^2\text{E}_1$) [25] and leads to well-resolved electron paramagnetic resonance (EPR) spectra even at room temperature.

Here, we report on the synthesis of the two new triradicals 1,3,5-tri([5]trovacenyl)benzene **4** and 1,3,5-tri([5]trovacenyl)-6-methoxybenzene **5** (Fig. 1). Furthermore, we investigated the electron spin-spin coupling in these equi-

lateral triangular triradicals by means of EPR spectroscopy and magnetic susceptometry [23].

2 Methods and Materials

All chemical manipulations were carried out under an atmosphere of argon or dinitrogen by Schlenk techniques. Physical measurements were performed with methods and instruments as specified previously [26]. EPR spectra were recorded on an ESP 300E continuous-wave (cw) X-band EPR spectrometer (Bruker) equipped with a rectangular cavity (Bruker) in combination with a liquid nitrogen cryostat and a temperature controller both from Oxford Instruments. Magnetic susceptibilities were studied with a superconducting quantum interference device susceptometer (Quantum Design) in the temperature range from 1.8 to 300 K. The data were corrected for magnetization of the sample holder (KLF), and diamagnetic corrections were applied to the magnetic susceptibility data on the basis of Pascal's constants. Trovacene **1** [27], phenyl-[5]trovacene **2** [20], 1,3-di([5]trovacenyl)benzene **3** [18], Pd(dppf)Cl₂ [28], and 1,3,5-triiodobenzene [29] were prepared as described in the literature. 2,4,6-Triidoanisole was purchased from Sigma. Anhydrous zinc chloride was obtained by melting ZnCl₂·4H₂O in vacuo.

1,3,5-Tri([5]trovacenyl)benzene (4). 300 mg of trovacene (TVC) **1** (1.4 mmol), dissolved in 50 ml of diethyl ether, were lithiated by 0.9 ml of a solution of n-BuLi in hexane (1.6 M) during 10 h at room temperature. The lithiated trovacene was then transmetalated by adding 1.6 ml of anhydrous ZnCl₂ in THF (0.9 M). 105 mg (0.23 mmol) of 1,3,5-triiodobenzene and 5 mg (6.8 μmol) of Pd(dppf)Cl₂ (dppf = 1,1'-bis(diphenylphosphino)ferrocene) were dissolved in 20 ml of THF, stirred for 30 min at room temperature and the resulting solution was injected into the TVCZnCl solution. The reaction mixture was refluxed for 1 h. Finally, the solvents were removed in vacuum, the residue was redissolved in 5 ml of toluene and subjected to column chromatography (size of column, 30 by 2.5 cm; Al₂O₃, 0% H₂O, benzene). The first band contained unreacted **1**, the second band, eluted with benzene/toluene 1:1, consisted of **4**, which was recrystallized from THF (5 ml) as a green powder. Yield: 139 mg (0.2 mmol, 87%). EIMS (70 eV) *m/z* (relative intensity, ion) 693 (100%, M⁺), 346 (15%, M²⁺). IR (KBr) $\tilde{\nu}_{\text{max}}$ (cm⁻¹): 3040 (weak), 1800–1600 (weak), 1594 (strong), 779 (strong), 455 (strong), 438 (medium), 413 (strong). Anal. Calcd. for C₄₂H₃₆V₃ (693.57 g/mol): C, 72.73; H, 5.23. Found: C, 72.75; H, 5.11.

1,3,5-Tri([5]trovacenyl)-6-methoxybenzene (5). Trovacene **1** (300 mg, 1.4 mmol), dissolved in 50 ml of diethyl ether, was lithiated by 0.9 ml of a solution of n-BuLi in hexane (1.6 M) during 10 h at room temperature. The lithiated trovacene was then transmetalated by adding 1.6 ml of a solution of anhydrous ZnCl₂ in THF (0.9 M). 112 mg (0.23 mmol) of 1,3,5-triidoanisole and 5 mg (6.8 μmol) of Pd(dppf)Cl₂ were dissolved in 20 ml of THF, stirred for 30 min at room temperature and injected into the TVCZnCl solution. The reaction mixture was refluxed for 1 h. Finally, the solvents were removed in vacuum, the residue was dissolved in 5 ml of benzene and subjected to column chromatog-

raphy (size of column, 30 by 2.5 cm; Al_2O_3 , 0% H_2O , benzene). The use of benzene as eluent yielded one fraction with unreacted trovacene **1**, while the product band immobilized 10 cm from the top to the column. Before the product fraction could be eluted from the column with THF, the residue on the very top of the column had to be removed mechanically. The product fraction was condensed to 10 ml, from which **5** crystallized at 0°C as long needles. Yield: 145 mg (0.2 mmol, 87%). EIMS (70eV) m/z (relative intensity, ion) 723 (100%, M^+), 616 (8%, $\text{M}^+ \cdot \text{C}_7\text{H}_7\text{-CH}_3$), 361.5 (17%, M^{2+}). IR (KBr) $\tilde{\nu}_{\text{max}}$ (cm^{-1}): 3038 (weak), 1800–1650 (weak), 1635–1427 (medium), 1260 (medium), 779 (strong), 431 (strong). Anal. Calcd. for $\text{C}_{43}\text{H}_{38}\text{OV}_3$ (723.60 g/mol): C, 71.37; H, 5.29. Found: C, 70.40; H, 4.66.

3 Results and Discussion

3.1 Synthesis

The new organometallic triradicals **4** and **5** were synthesized via selective lithiation of the five-membered ring of **1**, followed by transmetalation of Li-[5]trovacene with ZnCl_2 to yield ZnCl-[5]trovacene and subsequent $\text{Pd}(\text{dppt})\text{Cl}_2$ -catalyzed cross-coupling of ZnCl-[5]trovacene with 1,3,5-triiodobenzene or 2,4,6-triidoanisole, respectively (Fig. 1). The cross-coupling reaction, which follows a method developed by Negishi and Kumada [30], gives relatively high yields of about 87% with respect to the iodocompounds. The yields on the basis of **1** are, however, just about 14%, which is due to the yet unexplained fact that the lithiation of **1** stops at 50% conversion. Both products were purified by column chromatography and recrystallization. The crystals obtained were not suitable for X-ray analysis. Phenyl-[5]trovacene **2** [20] and 1,3-di([5]trovacenyl)benzene **3** [18], which are the mono- and biradical analogues of **4** and **5** were resynthesized for the sake of comparison of the magnetic data.

3.2 Triangular Spin System

The interaction between three spins S_1 , S_2 and S_3 localized at the corner of a triangle (Fig. 2a) can be described by the Heisenberg spin Hamiltonian given in Eq. (1) [5, 31] assuming that two interaction pathways, here S_1S_2 and S_1S_3 , are equal and are denoted as J , whereas the third interaction J' is different, the ratio of J'/J is α ,

$$\mathcal{H} = -2J(S_1S_2 + S_1S_3 + \alpha S_2S_3). \quad (1)$$

The relative energies of the spin states are $E_{\text{quartet}} = -J - J'/2$, $E_{\text{doublet},1} = 2J - J'/2$ and $E_{\text{doublet},2} = 3J'/2$ corresponding to the spin alignments as given in Fig. 2b–d, respectively. If the exchange coupling constants J and J' are positive, then the ground state of the spin system would be the quartet (Fig. 2b). However, if the coupling is antiferromagnetic, the spin alignment in the ground state depends on

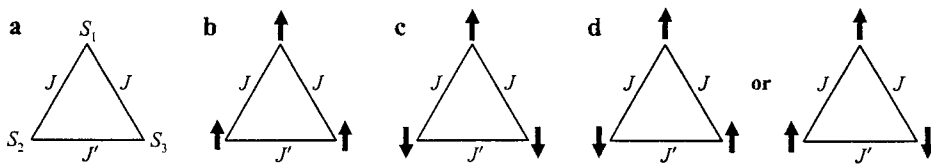


Fig. 2. Schematic of an exchange-coupled triangular system (a) with J and J' positive (b), J and J' negative and $|J| > |J'|$ (spin state doublet 1) (c), J and J' negative and $|J| < |J'|$ (spin state doublet 2) (d). c and d Competing interactions.

the value of α . For $\alpha < 1$ ($|J| > |J'|$) the spin ground state is the nondegenerate doublet 1 shown in Fig. 2c and for $\alpha > 1$ ($|J| < |J'|$) the lowest spin state is the nondegenerate doublet 2 (Fig. 2d). In both cases the two spins connected by the smaller J have to align parallel despite the antiferromagnetic exchange coupling between them, a situation which is called competing interactions. Spin frustration occurs if $J = J' =$ antiferromagnetic ($\alpha = 1$); in this case the system has a twofold degenerate doublet ground state ($E_{\text{doublet},1} = E_{\text{doublet},2} = 3J/2$). An example for an isosceles triangular trisnitroxide radical exhibiting competing interactions was established some time ago by Iwamura [31], and Pope et al. [32] discuss the effect of spin frustration for an inorganic triradical of equilateral triangular structure. Other examples of antiferromagnetically coupled inorganic and ferromagnetically coupled organic triradicals are collected in ref. 5.

3.3 EPR Spectroscopy

Initially, cw X-band EPR spectroscopy was applied in order to check whether the three unpaired electrons in **4** and **5** are exchange-coupled. In cases where $|J|$ is of the same order of magnitude as the isotropic hyperfine coupling constant A_{iso} , the magnitude of J may be determined from liquid-solution EPR spectra by analyzing the hyperfine pattern [18, 33]. The EPR spectra of the trovacene derivatives **2–5** in solution are collected in Figs. 3–5. Monoradical **2** (Fig. 3a) shows eight lines with a hyperfine coupling constant $A_{\text{iso}}(^{51}\text{V})$ of 71.8 G due to the coupling of the electron spin to the nuclear spin of ^{51}V ($I = 7/2$). Biradical **3** (Fig. 3b) exhibits a hyperfine pattern of 15 lines with a splitting of half the value observed for the monoradical **2**, indicative of the electron spin-spin coupling between two unpaired electrons centered on two nuclei of ^{51}V . Simulations yielded the value $|J| = 0.48(7)$ cm $^{-1}$ as already discussed in refs. 18 and 21. The two triradicals **4** (Fig. 4) and **5** (Fig. 5) display 22 lines with a splitting of 71.8 G/3 = 23.9 G, clearly demonstrating that the three unpaired electrons are interacting with each other and that $|J| > A_{\text{iso}}(^{51}\text{V})$. A simulation of the spectra, which might have specified the magnitudes of the exchange coupling constants, was impractical because the computational time to treat three interacting nuclei of ^{51}V is prohibitively large as yet. Interestingly, however, the intensity distribution of the lines in the two spectra differs, which points to a different extent of exchange

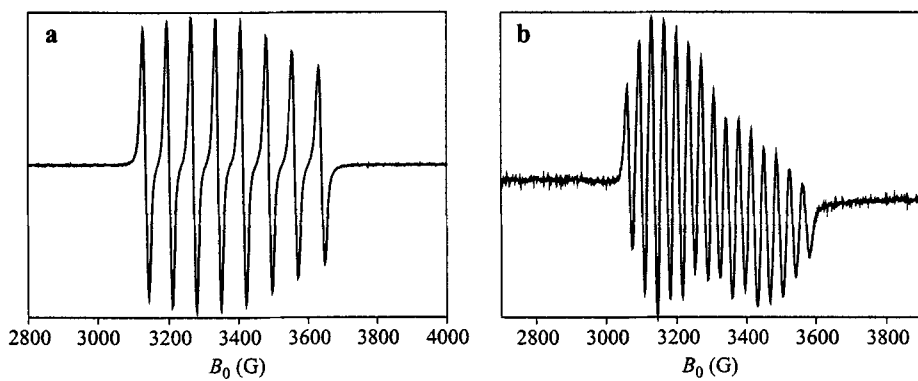


Fig. 3. EPR spectra of **2** (a) and **3** (b) at 295 K both in toluene. Microwave power, 1 mW; conversion time and time constant, 20 ms; modulation amplitude, 1 G; modulation frequency, 100 kHz; receiver gain, $1 \cdot 10^4$.

coupling in both complexes. In frozen solution ($T = 100$ K) neither **4** nor **5** (Figs. 4b and 5b) show signals at $g = 4$ or $g = 6$. For **3** a half-field signal could neither be detected. In all three cases this must be attributed to the fact that the exchange coupling is too small and the distances between the spins are too large to yield half-field and third-field signals of sufficient intensity to be detected at this temperature.

3.4 Magnetic Susceptibility Measurements

Information concerning the magnitude and the sign of J could be gained from temperature-dependent measurements of the bulk magnetic susceptibility χ of mi-

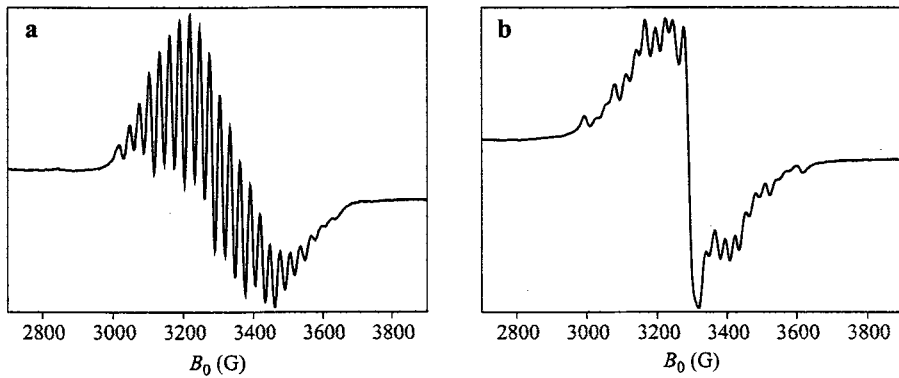


Fig. 4. EPR spectra of **4** in toluene at 295 K (a) and 100 K (b). Microwave power, 1 mW; conversion time and time constant, 20 ms; modulation amplitude, 1 G; modulation frequency, 100 kHz; receiver gain, $1 \cdot 10^4$.

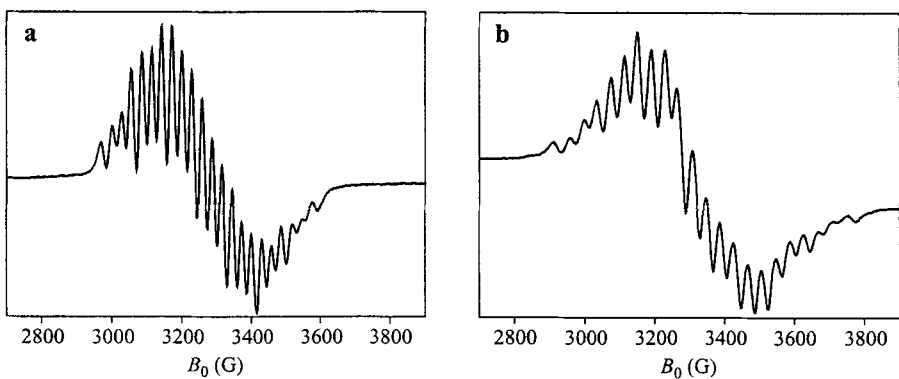


Fig. 5. EPR spectra of **5** in toluene at 295 K (a) and 100 K (b). Microwave power, 1 mW; conversion time and time constant, 20 ms; modulation amplitude, 1 G; modulation frequency, 100 kHz; receiver gain, $1 \cdot 10^4$.

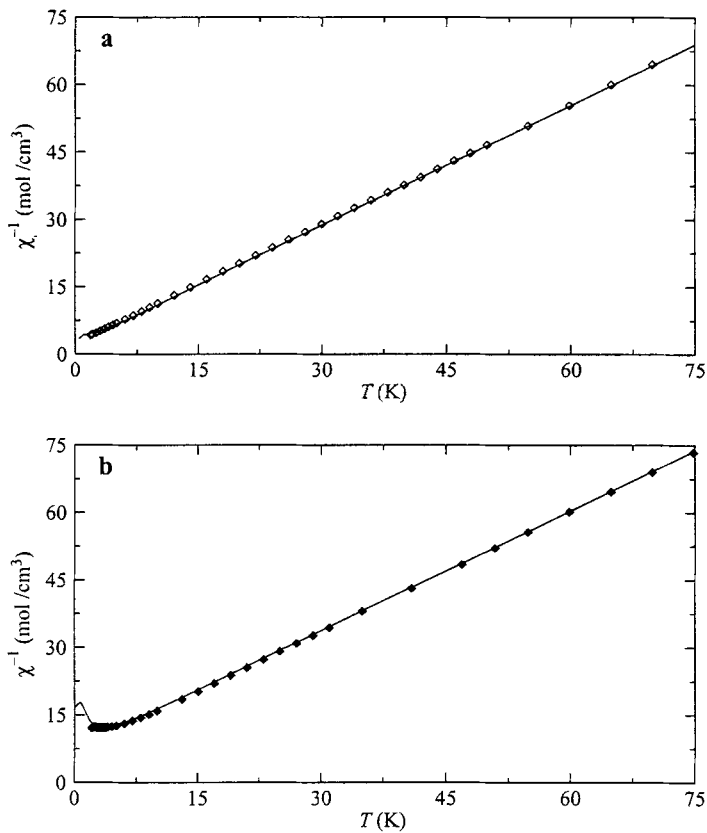


Fig. 6. Plots of χ^{-1} over T for **4** (a) and **5** (b). The solid lines are the fits to the data points. For fitting formula see text.

cocrystalline powders of **4** and **5**. The plots of χ^{-1} over T are shown in Fig. 6. At temperatures above 50 K the data could be fitted to the Curie-Weiss law with values for the Curie-Weiss temperatures Θ of $-0.8(2)$ K and $-6.0(6)$ K and with Curie-Weiss constants C of $1.07 \text{ cm}^3 \text{K/mol}$ and $1.07 \text{ cm}^3 \text{K/mol}$ for **4** and **5**, respectively. The value derived for the magnetic moments μ_C of $2.92\mu_B$ for both complexes corresponds to a magnetic moment μ_V per vanadium atom of $1.68(3)\mu_B$, which is close to the spin-only value of $1.73\mu_B$ for one unpaired electron per vanadium atom.

All data points, including the points below 50 K, were fitted (solid line in Fig. 6) according to Eq. (2), which was derived by Iwamura [31] and is based on the model described in Sect. 2.3:

$$\chi = \frac{3 \cdot N_A \cdot \mu_B^2 \cdot g^2}{12kT} \cdot \frac{1 + \exp(2(\alpha - 1)J/T) + 10 \cdot \exp(1 + 2\alpha) \cdot J/T}{1 + \exp(2(\alpha - 1)J/T) + 2 \cdot \exp(1 + 2\alpha) \cdot J/T} \cdot \frac{T}{T - \Theta}. \quad (2)$$

The symbols have their usual meaning and g was taken from the EPR spectra as 1.998 for **4** and **5**. It should be noted that both fits are unique solutions and that no other solution fit the data as well, in contrast to cases studied by Iwamura [31] and Hendrickson [34]. The experimental data points of **4** could be fitted best with $J = -0.68(1) \text{ cm}^{-1}$ and $\alpha = 1$, meaning that the coupling is antiferromagnetic and that **4** shows the effect of spin frustration (twofold degenerate spin ground state [$E_{\text{doublet},1} = E_{\text{doublet},2} = 0$]). The exchange coupling is much weaker than that for the biradical analog **3** with $J = -1.67(4) \text{ cm}^{-1}$, which is most probably caused by the spin frustration as also observed for the pair mesityl-di([5]trovacenyl)borane/tri([5]trovacenyl)borane [19]. This analogy is based on the premise that in both **3** and **4** the trovacenyl sandwich axes are normal to the arene plane of the bridging unit. While for **3** this has been established by X-ray diffraction, for **4** no structural data are available as yet. It may be safely assumed, however, that **4** is isostructural with tri(ferrocenyl)borazine $\text{Fc}_3\text{B}_3\text{N}_3$ [35], tri(ferrocenyle)boroxime $\text{Fc}_3\text{B}_3\text{O}_3$ [35] and tri(ferrocenyle)borselenin $\text{Fc}_3\text{B}_3\text{Se}_3$ [36] all of which possess structures analog to that proposed for **4** in Fig. 1.

Methoxy substitution at position 6 of the benzene ring in **5** raises the C_3 symmetry and thereby leads to two differing pathways with exchange coupling constants of $J = -1.83(5) \text{ cm}^{-1}$ and $J' = -2.38(8) \text{ cm}^{-1}$ ($\alpha = 1.35$). Clearly, the antiferromagnetic coupling prevails, but the degeneracy of the ground state found in **4** is removed, leaving doublet 2 (Fig. 2d) as the lowest spin state. Thus the effect of competing interactions is present in **5**. Due to symmetry reasons, J' is assigned to the coupling between the trovacenyl groups in position 1 and 5 of the benzene ring (for numbering scheme, see Fig. 1), which is the pathway altered by the methoxy substituent, whereas the two equal couplings J are those between trovacenyl units at positions 1 and 3 and 3 and 5, which are separated by unsubstituted CH units. Furthermore, since the ratio of J'/J is larger than 1, the spins on the trovacene moieties in position 1 and 5 have to be aligned antiferromagnetically, whereas the spin on the trovacene substituent in position 3 must align in a ferromagnetic fashion to one of the two spins in positions 1 and 5 (Fig. 2d).

Interestingly, the exchange coupling $J = -1.83 \text{ cm}^{-1}$ in **5** is very similar to that found for **3** ($J = -1.67 \text{ cm}^{-1}$), which supports the proposal of similar cyclopentadienyl/benzene dihedral angles in **5** and **3**. However, the presence of the methoxy substituent in the exchange coupling pathway characterized by J' leads to a considerable increase of exchange coupling, $J'(\mathbf{5}) = -2.38 \text{ cm}^{-1}$ versus $J(\mathbf{3}) = -1.67 \text{ cm}^{-1}$, which must be attributed to electronic changes imposed by the methoxy group.

Finally, the mechanisms for the exchange coupling should be addressed. For both complexes **4** and **5** a through-space interaction of the spins is probably insignificant, considering the large distance between the vanadium atoms, $d(\text{V-V}, \mathbf{3}) = 0.72 \text{ nm}$. Conversely, taking into account the sensitivity of the exchange interaction to a substitution at bridging atoms, a through-bond mechanism appears plausible. Through-bond coupling most likely proceeds via the combined action of spin polarization and superexchange [9, 18–23]. Yet, both mechanisms lack efficiency [37], which manifests itself in the small hyperfine coupling constants of the hydrogen nuclei at the coordinated rings, $A_{\text{iso}}(^1\text{H}_{\text{cp}}) = 1.8 \text{ G}$ [38]. This lack of efficiency also explains why the exchange coupling for trovacene derivatives is relatively small, compared to bisnitroxides [31] or other inorganic compounds [5]. In addition, this combination of mechanisms might also be the reason for the antiferromagnetic coupling via the *meta*-substituted bridge, because it is believed that the ferromagnetic coupling properties of this bridge rely on spin polarization [5]. Another reason could be that the cyclopentadienyl rings have to be included into the bridge, which makes the whole group a non-alternating hydrocarbon and hence a bridge with antiferromagnetic coupling properties.

3.5 Cyclovoltammetric Measurements

In addition to exchange interactions J between multiple paramagnetic sites, an effect which can be paraphrased as magnetocommunication, there is also electrocommunication, which deals with the influence which oxidation or reduction at one of these sites exerts on subsequent redox processes of the same molecule. The parameter of interest here is the redox splitting $\delta E_{1/2}$, which is the potential difference between subsequent redox steps, $\delta E_{1/2} = 0$ implying no interaction between the redox centers. Since magneto- and electrocommunication probably rely on different mechanisms, it is of interest to compare J and $\delta E_{1/2}$ values for a certain set of molecules.

The cyclovoltammetric (CV) traces for **4** and **5** are displayed in Fig. 7, the experimental parameters are collected in Table 1. In line with the frontier orbital sequence $e_2^4a_1^1e_1^0$ for trovacene **1** and with the dominance of the $\text{V}(3d_{z^2})$ orbital in the MO a_1 , oxidation and reduction of derivatives of **1** are metal-centered. As gleaned from Fig. 7, the three consecutive oxidation steps for both **4** and **5** occur practically at the same potential ($\delta E_{1/2} < 50 \text{ mV}$). For the reduction processes, however, **4** and **5** display three resolved and reversible redox

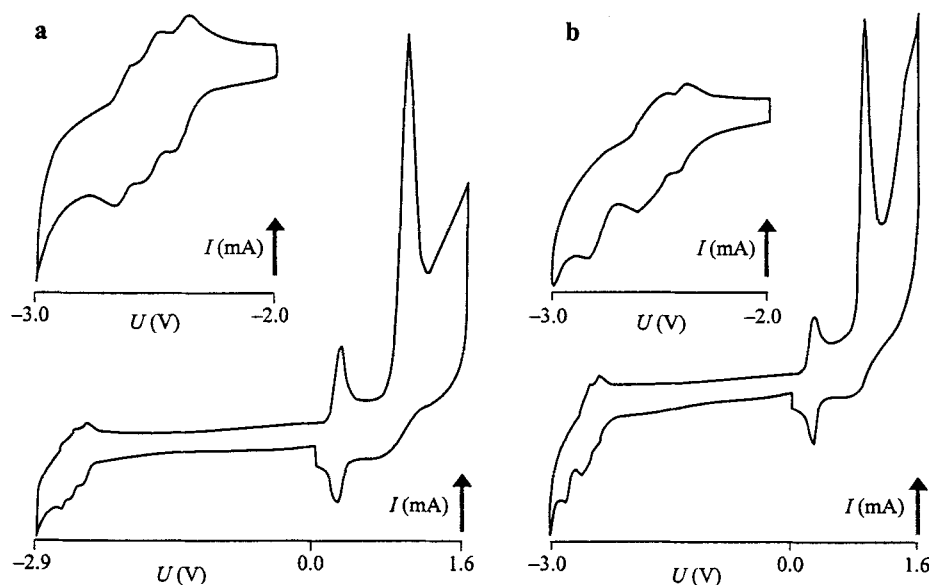


Fig. 7. Cyclic voltammetric traces for 1,3,5-tri([5]tropocyclonaphthalene)benzene **4** and 1,3,5-tri([5]tropocyclonaphthalene)-6-methoxybenzene **5**. The measurements were performed in dimethoxyethane at -40°C . The reference electrode was a saturated calomel electrode and the potential was varied with a velocity of 0.1 Vs^{-1} .

Table 1. Electrochemical data from cyclovoltammetry performed on triradicals **4** and **5**.

Parameter ^a	4	5
$E_{1/2}(0/3+)$ (V)	+0.266	+0.293
ΔE_p (mV)	59	78
I_{pa}/I_{pc}	3/3	3/3
$\delta E_{1/2}(0/3+)$ (mV)	≤ 50	≤ 50
$E_{pa}(3+/4+)$ (V)	+1.0	+1.0
$E_{1/2}(0/-)$ (V)	-2.404	-2.398
ΔE_p (mV)	64	59
I_{pa}/I_{pc}	1/1	1/1
$E_{1/2}(-2/-)$ (V)	-2.518	-2.514
ΔE_p (mV)	67	60
I_{pa}/I_{pc}	1/1	1/1
$\delta E_{1/2}(0/-)/(-2/-)$ (mV)	114	114
$E_{1/2}(2/-3-)$ (V)	-2.632	-2.585
ΔE_p (mV)	66	59
I_{pa}/I_{pc}	1/1	1/1
$\delta E_{1/2}(-2/-)/(2/-3-)$ (mV)	114	72
$E_{pc}(3/-4-)$ (V)	—	-2.834

^a $E_{1/2}$ is the thermodynamic potential of the redox event; ΔE_p is the potential difference between the anodic and cathodic current maxima; I_{pa} and I_{pc} are the anodic and cathodic peak current, respectively; $\delta E_{1/2}$ is the redox splitting.

steps. The oxidation-reduction disparity can be rationalized by the fact that metal-metal or metal-ligand interaction will be weakened upon metal-centered oxidation, because of attendant metal-orbital contraction, but increased upon reduction due to metalorbital expansion.

The two equal redox splittings of $\delta E_{1/2} = 114$ mV for complex **4** reflect the C_3 symmetry of the complex, whereas the lowering of the symmetry, induced by the methoxy substituent, leads to two differing redox splittings of $\delta E_{1/2} = 114$ mV and 72 mV for complex **5**. The equality of $E_{1/2}(0/-)$ and of $\delta E_{1/2}(0/-, -/2-)$ for **4** and **5** suggests that the first electron in the reduction chain of **5** is transferred to the trovacyl group linked to C-3. The third step in the reduction of **5**, $E_{1/2}(2-/3-)$, however, occurs at a less negative potential than the step $E_{1/2}(2-/3-)$ of **4** and 12 the redox splitting $\delta E_{1/2}(-/2-, 2-/3-)$ is reduced to 72 mV, pointing to the fact that electrocommunication between the trovacyl groups at C-1 and C-5 is attenuated compared with the communication between the trovacyl groups at C-3/C-5 or C-3/C-1. To explain this finding, concepts on the basis of a through-bond as well as on a through-space mechanism can be put forward. In the through-bond variant it could be argued that substitution of H for OCH₃ increases *ortho*-compression strain and leads to larger twist angles between the η^5 -cyclopentadienyl and bridging benzene planes thereby reducing π -conjugation. In the through-space variant it is conceivable that the change in dielectric properties upon replacing H by OCH₃ in the region between the redox centers weakens the electrostatic interaction.

4 Conclusion

It may be stated that both magneto- and electrocommunication in a triangular system comprised of open-shell redox-active groups are affected by symmetry lowering substitution at an initially C_3 -symmetric bridging unit; the perturbation clearly manifested itself in the result of susceptometric and cyclovoltammetric studies. In the system under study here the introduction of a methoxy group between two *ortho*-positioned [5]trovacyl moieties has inverse effects in that exchange coupling J is strengthened and redox splitting $\delta E_{1/2}$ is weakened. Attempts to attribute this discrepancy to the respective mechanisms of interaction are complicated by the fact that magnetic susceptometry was performed on a solid sample and cyclic voltammetry on molecules in fluid solution, the torsional angles $\eta^5\text{-C}_5\text{H}_4/\text{C}_6\text{H}_4$ being ill-defined in the latter.

Acknowledgements

This work has been supported by the Volkswagen Foundation and the Fonds der Chemischen Industrie.

References

1. Gatteschi D., Kahn O., Miller J.S., Palacio F. (eds.): *Magnetic Molecular Materials*. NATO ASI Series, series N, vol. 198. Dordrecht: Kluwer Academic 1991.
2. Miller J.S., Drillon M. (eds.): *Magnetism: Molecules to Materials*. Weinheim: Wiley-VCH 2002.
3. Bencini A., Gatteschi D.: *Electron Paramagnetic Resonance of Exchange Coupled Systems*, chapt. 9. Berlin: Springer 1990.
4. Borden W.T. (ed.): *Diradicals*. New York: Wiley 1982.
5. Kahn O.: *Molecular Magnetism*. Weinheim: Wiley-VCH 1993.
6. Kokorin A.I.: *Appl. Magn. Reson.* **26**, 253–274 (2004)
7. Saladino A.C., Larsen S.C.: *J. Phys. Chem. A* **107**, 4735–4740 (2003)
8. Barlow S., O'Hare D.: *Chem. Rev.* **97**, 637–670 (1997)
9. Elschenbroich C., Plackmeyer J., Harms K., Burghaus O., Pebler J.: *Organometallics* **22**, 3367–3373 (2003)
10. Lathi P.M. (ed.): *Magnetic Properties of Organic Materials*. New York: Marcel Dekker 1999.
11. Elschenbroich C., Metz B., Neumüller B., Reijerse E.: *Organometallics* **13**, 5072–5079 (1994)
12. Ishida T., Iwamura H.: *J. Am. Chem. Soc.* **113**, 4238–4241 (1991)
13. Rajca A., Rajca S., Desai S.R.: *J. Am. Chem. Soc.* **117**, 806–816 (1995)
14. Matsuda K., Nakamura N., Inoue K., Koga N., Iwamura H.: *Chem. Eur. J.* **2**, 259–264 (1996)
15. Okada K., Imakura T., Oda M., Murai H., Baumgarten M.: *J. Am. Chem. Soc.* **118**, 3047–3048 (1996)
16. West A.P., Silverman S.K., Dougherty D.A.: *J. Am. Chem. Soc.* **118**, 1452–1463 (1996)
17. Dvořá茨ky M., Chiarelli R., Rassat A.: *Angew. Chem. Int. Ed.* **31**, 180–181 (1992)
18. a) Elschenbroich C., Wolf M., Schiemann O., Harms K., Burghaus O., Pebler J.: *Organometallics* **21**, 5810–5819 (2002); b) Burghaus O., Schiemann O., Wolf M., Plackmeyer J., Elschenbroich C. in: *Proceedings of the Joint 29th AMPERE – 13th ISMAR* (Ziessow D., Lubitz W., Lendzian F., eds.), p. 1186. Berlin: Technische Universität Berlin 1998.
19. Elschenbroich C., Wolf M., Burghaus O., Harms K., Pebler J.: *Eur. J. Inorg. Chem.* **12**, 2173–2185 (1999)
20. Elschenbroich C., Schiemann O., Burghaus O., Harms K., Pebler J.: *Organometallics* **18**, 3273–3277 (1999)
21. Elschenbroich C., Schiemann O., Burghaus O., Harms K., Pebler J.: *J. Am. Chem. Soc.* **119**, 7452–7457 (1997)
22. Elschenbroich C., Bilger E., Metz B.: *Organometallics* **10**, 2823–2827 (1991)
23. Schiemann O.: Ph.D. thesis, Phillips University of Marburg, Marburg, Germany, 1998.
24. Groenenboom J.C., DeLiefde H.J., Jellinek F.: *J. Organomet. Chem.* **69**, 235–240 (1974)
25. Elschenbroich C.: *Organometallchemie*, 4th edn. Wiesbaden: Teubner 2003.
26. Elschenbroich C., Voss S., Schiemann O., Lippe A., Harms K.: *Organometallics* **17**, 4417–4424 (1998)
27. King R.B., Stone F.G.A.: *J. Am. Chem. Soc.* **81**, 5263–5264 (1959)
28. Hayashi T., Konishi M., Kumada M.: *Tetrahedron Lett.* **21**, 1871–1874 (1979)
29. Willgerodt C., Arnold E.: *Chem. Ber.* **34**, 3345–3358 (1901)
30. Knochel P., Jones P. (eds.): *Organozinc Reagents: A Practical Approach*, chapt. 11. Oxford: Oxford University Press 1999.
31. Fujita J., Tanaka M., Suemune H., Koga N., Matsuda K., Iwamura H.: *J. Am. Chem. Soc.* **118**, 9347–9351 (1996)
32. Woo H.Y., So H., Pope M.T.: *J. Am. Chem. Soc.* **118**, 621–626 (1996)
33. Shiomi D., Kaneda C., Kanaya T., Sato K., Takui T.: *Appl. Magn. Reson.* **23**, 495–506 (2003)
34. McCusker J.K., Vincent J.B., Schmitt E.A., Mino M.L., Shin K., Coggins A.K., Hagen P.M., Huffman J.C., Christou G., Hendrickson D.N.: *J. Am. Chem. Soc.* **113**, 3012–3021 (1991)
35. Bats J.W., Ma K., Wagner M.: *Acta Crystallogr. C* **58**, m129 (2002)
36. Horn H., Rudolph F., Ahlrichs R., Merzweiler K.: *Z. Naturforsch. B* **47**, 1 (1992)
37. LaMar G.N., Horrocks W.W., Holm R.H. (eds.): *NMR of Paramagnetic Molecules: Principles and Applications*, chapt. 6. New York: Academic Press 1973.
38. Rettig M.F., Stout C.D., Klug A., Farnham P.: *J. Am. Chem. Soc.* **92**, 5100–5104 (1970)

Authors' address: Olav Schiemann, Institut für Physikalische und Theoretische Chemie, J. W. Goethe-Universität, Marie-Curie-Strasse 11, 60439 Frankfurt am Main, Germany
E-mail: o.schiemann@prisner.de